An atypical haem in the cytochrome b_6f complex

David Stroebel[1], Yves Choquet[2], Jean-Luc Popot[1] & Daniel Picot[1]

[1]*Laboratoire de Physico-Chimie Moléculaire des Membranes Biologiques, CNRS/Université Paris 7, UMR 7099,* [2]*Laboratoire de Physiologie Membranaire et Moléculaire du Chloroplaste, CNRS UPR 1261, Institut de Biologie Physico-Chimique, 13 rue Pierre et Marie Curie, F-75005 Paris, France*

Photosystems I and II (PSI and II) are reaction centres that capture light energy in order to drive oxygenic photosynthesis; however, they can only do so by interacting with the multisubunit cytochrome b_6f complex. This complex receives electrons from PSII and passes them to PSI, pumping protons across the membrane and powering the Q-cycle. Unlike the mitochondrial and bacterial homologue cytochrome bc_1, cytochrome b_6f can switch to a cyclic mode of electron transfer around PSI using an unknown pathway. Here we present the X-ray structure at 3.1 Å of cytochrome b_6f from the alga *Chlamydomonas reinhardtii*. The structure bears similarities to cytochrome bc_1 but also exhibits some unique features, such as binding chlorophyll, β-carotene and an unexpected haem sharing a quinone site. This haem is atypical as it is covalently bound by one thioether linkage and has no axial amino acid ligand. This haem may be the missing link in oxygenic photosynthesis.

Cytochrome b_6f (plastohydroquinone:plastocyanin oxidoreductase) and its partial homologue cytochrome bc_1 are thought to use a similar mechanism, the so-called Q-cycle[1,2], to couple electron transfer (from a hydroquinone to a cytochrome or plastocyanin) with proton translocation in order to generate a transmembrane electrochemical H^+ gradient ($\Delta\mu H^+$). Central to this mechanism is the two-electron oxidation of hydroplastoquinone coupled with the release of two protons at the Q_o site on one side of the membrane (the lumen in chloroplasts). One electron is transferred through a high-potential chain comprising an Fe_2S_2 cluster and a haem *f*, analogous to c_1 in cytochrome bc_1, whereas the other is directed through haems b_L and b_H to reduce quinone at the Q_i site on the other side of the membrane (the stroma in chloroplasts); upon two successive reduction events at the Q_i site, two protons are taken up from the stroma. Thus $\Delta\mu H^+$ is generated through the release and uptake of protons on either side of the membrane.

Cytochromes bc_1 and b_6f have fundamental differences despite their mechanistic similarities. In oxygenic photosynthesis the electron pathway can switch from a linear mode, which starts with water and ends with NADPH, to a cyclic one, where electrons transferred from cytochrome b_6f to PSI, on the luminal face of the membrane, are fed back to b_6f on the stromal face, boosting ATP synthesis at the expense of reducing equivalents. This re-injection pathway is not understood. It may involve an NADH-plastoquinone reductase[3], or may be mediated directly by ferredoxin, the ferredoxin:$NADP^+$ oxidoreductase[4], or by a biochemically unidentified G cytochrome[5,6]. Furthermore, b_6f is thought to regulate state transitions by activating a protein kinase[7,8]. A b_6f-specific proton-pumping mechanism has also been proposed[9]. Finally, two cofactors of unknown function, chlorophyll *a* and β-carotene, are part of cytochrome b_6f[10].

The X-ray structures of mitochondrial cytochrome bc_1[11–14] have provided a structural framework for modelling cytochrome b_6f.

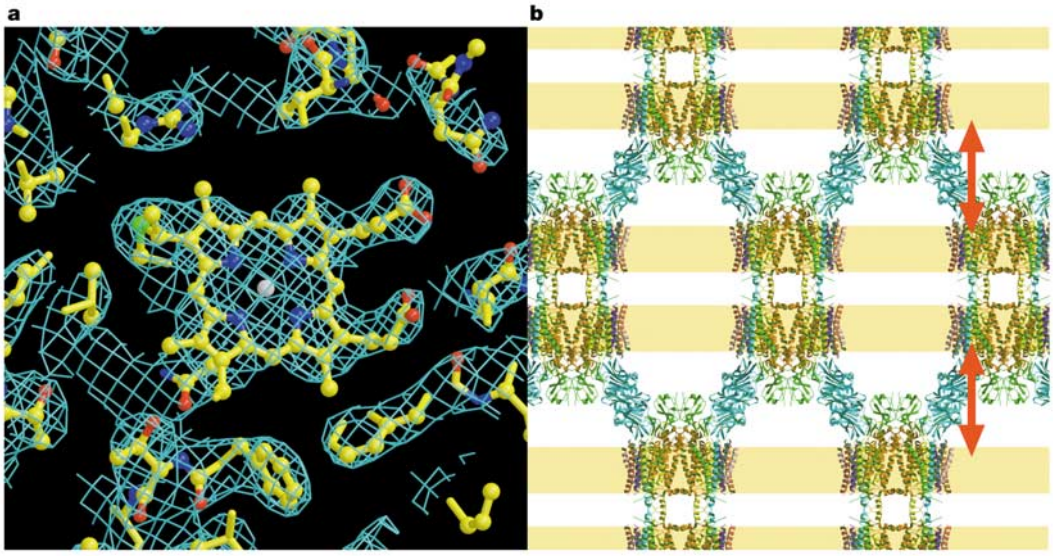

Figure 1 Crystallography of b_6f complex. **a**, Electron density of haem c_i in the Q_i site. ($2F_o - F_c$)-weighted map contoured at the 2σ level. Yellow, carbon; red, oxygen; blue, nitrogen; grey, iron. **b**, Crystal packing. A view normal to the molecular two-fold axis shows successive layers corresponding to stromal, transmembrane (in yellow) and luminal (delimited with red arrows) regions of the complex. In the latter, contacts between layers involve exclusively cytochrome *f*. The thickness of the 'luminal' space (red arrow, 70 Å) is close to that measured in thylakoids[51]. The molecular two-fold axis is a crystallographic axis, and the crystal contains one monomer per asymmetric unit.

This has given useful insights into the Q_o site of b_6f, but puzzling results for Q_i. The X-ray structure (Table 1) of the b_6f complex described here explains these discrepancies and provides new clues for the understanding of oxygenic photosynthesis.

General polypeptide arrangement

The b_6f complex has a strong tendency to dissociate in detergent solution[15]. This problem has been overcome by the design of a rapid purification scheme using low detergent concentration, requiring less than a day from purification to crystallization assays. This procedure avoids adding exogenous lipids[16,17]. The electron density map shown in Fig. 1 reveals all known subunits and cofactors plus several lipids.

The crystal structure shows a dimer (Figs 1b, 2 and 3) whose organization is similar to that of cytochrome bc_1, as already suggested[18]. The extramembrane domains of cytochrome *f* and the Rieske protein lie on the luminal side. Although cytochromes *f* (ref. 19) and c_1 share no structural similarity, they occupy roughly equivalent positions in the two complexes. However, the *c*-type haem of cytochrome *f* is shifted by 16.3 Å relative to that of cytochrome c_1. The extramembrane region of the Rieske protein is thought to be highly mobile[12,13,20]. In the dimer the two cytochrome *f* subunits, which make no contact, form a bowl-like structure that, *in situ*, protects the movement of the two Rieske proteins from interactions in the narrow luminal space (Figs 1b and 2a). The electron density is well defined for the Fe_2S_2-binding domain, but not for the other extramembrane domains, probably due to their mobility; however, with the exception of the link (residues 72–79) to the transmembrane helix, they can be localized[21]. The position of the Fe_2S_2 domain relative to the complex superimposes with that of the homologous domain in cytochrome bc_1 structures that binds stigmatellin[14] (Fig. 3).

The transmembrane region

There are 13 transmembrane helices per monomer (Fig. 2b, c). Those of cytochrome b_6 and subunit IV exhibit a high degree of similarity to their homologues in the bc_1 cytochrome. The insertion of an additional residue (Val 190) between the two haem-liganding histidines on helix D produces limited local perturbations. The tilt of the helices relative to the membrane plane creates, as in cytochrome bc_1, a groove at the dimer interface, thought to favour transfer of quinone between Q_o and Q_i. The single transmembrane helices of the Rieske protein and cytochrome *f* occupy equivalent locations to their counterparts in the bc_1 complex, but that of the Rieske protein is bent.

Table 1 **Summary of data collection and refinement statistics**

Summary statistics	Values
Data collection	
Wavelength (Å)	1.0080
Unit cell dimensions (Å)	102.35, 171.15, 351.91
Maximum resolution (Å)	3.1
Unique reflections	56,687
Completeness (%)	99.6 (99.6)
Redundancy	4.3
R_{sym}	0.089 (0.39)
I/σ	6.8 (1.8)
Refinement	
Resolution range (last shell) (Å)	35–3.1 (3.21–3.10)
Number of atoms	7,820
R_{work}/R_{free}	0.22 (0.34)/0.26 (0.36)
Deviation from ideal geometry	
R.m.s. bonds (Å)/r.m.s. angle (°)	0.008/1.32
R.m.s. dihedral (°)/r.m.s. improper (°)	19.8/3.0
Average *B* factors (Å^2)	69.9

$R_{sym} = \Sigma|I - \langle I\rangle|/\Sigma I$, *where* I is the intensity. $R_{work} = \Sigma||F_o| - |F_c||/\Sigma|F_o|$, where F_o and F_c represent the observed and calculated structure factor amplitudes. R_{free} is calculated from about 5% of randomly chosen reflections, which are not used in the refinement. R.m.s., root mean square. Values in parentheses refer to the highest resolution shell.

The four small subunits PetG, PetL, PetM and PetN form an approximate four-helix bundle, which has no counterpart in cytochrome bc_1. Conversely, helix H of cytochrome *b* and the small subunits su10, su7 and su11 (ref. 13) of bc_1 have no equivalent in cytochrome b_6f. Therefore, the two complexes feature different overall cross-sections (Fig. 2), with the small subunits of cytochrome b_6f occupying what in bc_1 is a large groove partially filled with specific lipids[22].

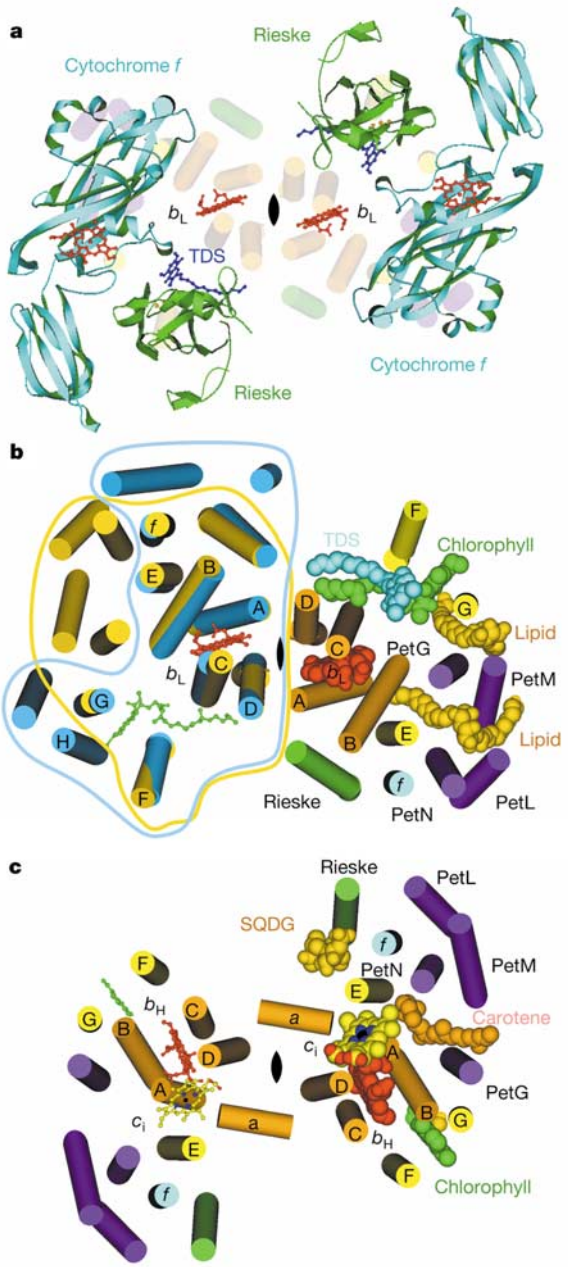

Figure 2 Three views of b_6f normal to the membrane. **a**, The lumen with cytochrome *f* and the Rieske protein. **b**, The transmembrane region viewed from the lumen. On the left, the transmembrane helices of cytochrome b_6f (yellow) are superimposed over those of cytochrome bc_1 (PDB entry 1BE3 (ref. 13); blue). The cross-section profile of the cytochrome bc_1 monomer is outlined in blue and that of cytochrome b_6f in yellow. On the right (cytochrome b_6 in orange, subunit IV in yellow and small subunits in purple), luminal cofactors and ligands are depicted in a space-filling representation. **c**, The stromal half of the transmembrane region viewed from the stroma (colours as in **b**). Helices are named according to cytochrome bc_1 terminology[12]: A, B, C and D for cytochrome b_6; E, F and G for subunit IV; helix H is present only in cytochrome *b*.

Chlorophyll

Chlorophyll *a* is a component of the b_6f complex[10]. Its chlorin ring is located between helices F and G of subunit IV (Fig. 2b, c), at the centre of the transmembrane region, in a space left accessible by the absence of a homologous helix H, which is present in mitochondrial cytochrome *b*. On both faces of the ring there are weak electron densities that can be attributed to lipids or other lipophilic compounds. No clear axial ligand can be seen, although electron density extends away from the chlorin plane, towards the carbonyl group of Gly 136 of subunit IV. The distance is too large (4.7 Å) for direct coordination, suggesting an intervening water molecule. The phytyl chain ends within the Q_o pocket.

β-carotene

β-carotene co-purifies with cytochrome b_6f[10,23]. One cyclohexene ring is deeply embedded not far (approximately 6.2 Å) from haem c_i (see below), whereas the other ring disappears from the electron density map at the protein–lipid interface (between PetG and PetM). A good fit to the electron density is observed with a 9-*cis*-β-carotene, in agreement with Raman spectra[24]. The β-carotene molecule seems too distant (14 Å) from the chlorophyll to efficiently quench singlet oxygen, in agreement with spectroscopic data[25], but it could interact with the Q_i site. The presence of additional carotenoids interacting with the chlorophyll *in situ* cannot be ruled out, as the edge of the chlorophyll is exposed to the lipid phase.

Specific features of cytochrome b_6f—the plastocyanin-binding site of cytochrome *f* (ref. 26), the small subunits helix bundle, the chlorophyll and the β-carotene—are all facing in the same direction out of the complex. This suggests that they could interact with other components of the photosynthetic apparatus, such as PSI or a kinase. The chlorophyll might serve as a sensor that connects the interacting partner with the Q_o site. The β-carotene might have a similar role at the Q_i site; however, other hypotheses[10] cannot be ruled out.

Endogenous lipids

On the stromal side lies a sulpholipid (sulphoquinovosyldiacylglycerol; SQDG) with partially visible fatty acyl chains (Fig. 2c). The head group electron density is well defined, and the sulphur atom produces a peak in an anomalous Fourier map. The sulphonate group interacts with Lys 272 at the stromal end of the transmembrane helix of cytochrome *f*. This lysine is involved in regulation of cytochrome *f* biosynthesis[27]. The luminal side features two lipids (probably monogalactosyldiacylglycerol; Fig. 2b)—two acyl chains with well-defined electron densities are embedded in the protein, in contact with β-carotene in one case and chlorophyll *a* in the other. The other acyl chains, partially disordered, lie at the lipid–protein interface.

Q_o and tridecylstigmatellin-binding sites

The luminal face harbours the high-potential chain and haem b_L of the low-potential chain. The Q_o site (Fig. 4), where hydroplastoquinone oxidation and proton release take place, is reminiscent of the bc_1 Q_o site; that is, it exhibits the same bifurcated volume, with its lobe distal from haem b_L occupied by the head group of the inhibitor tridecylstigmatellin (TDS). The entrance to the active site is partially occupied by the phytyl chain of the chlorophyll. Less bulky side chains at the opposite wall of the cleft compensate for the presence of the phytyl chain. This reorganization imposes onto the tail of TDS a shift of about 4 Å relative to that of stigmatellin in cytochrome bc_1[22]. The His 155 residue of the Rieske protein is within hydrogen-bonding distance of the carbonyl of the chromone ring, the suggested path for the release of one proton[12]. Differences exist in the lobe proximal to haem b_L. For instance, the side chain of Glu 78 of subunit IV (Glu 272 in yeast cytochrome *b*) has a poorly resolved electron density, suggesting mobility, whereas in bc_1 this residue has been proposed to have an important role in the release of the other proton[28]; its substitution by polar or basic residues in *C. reinhardtii* suggests that it is not essential for b_6f activity[29]. In the

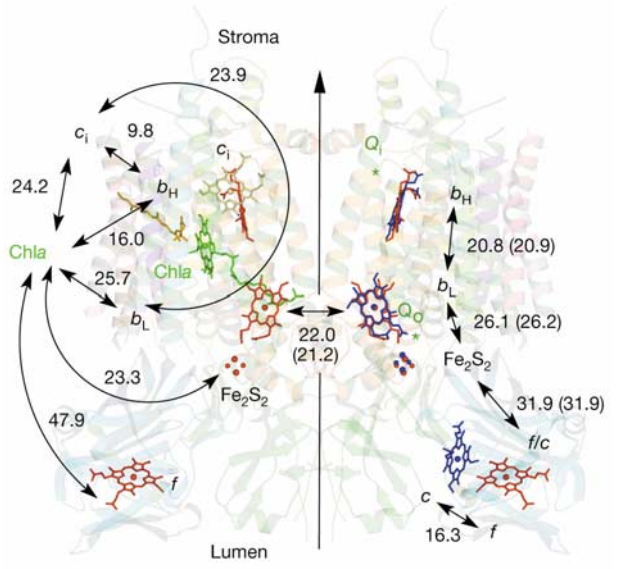

Figure 3 Cofactors in the dimer. Cytochrome b_6f's haems (red, haem c_i in yellow), Fe_2S_2 (red) and chlorophyll (green) are represented as viewed along the membrane plane. On the right, the cofactors of cytochrome bc_1 (blue) are superimposed (PDB entry 1KB9; ref. 22). Distances between metal centres (in Å) are indicated for cytochrome b_6f and are in parentheses for cytochrome bc_1. The angle between the planes of haem c_i and b_H is 74°; the iron of haem c_i is 3.9 Å closer to the stroma than that of b_H.

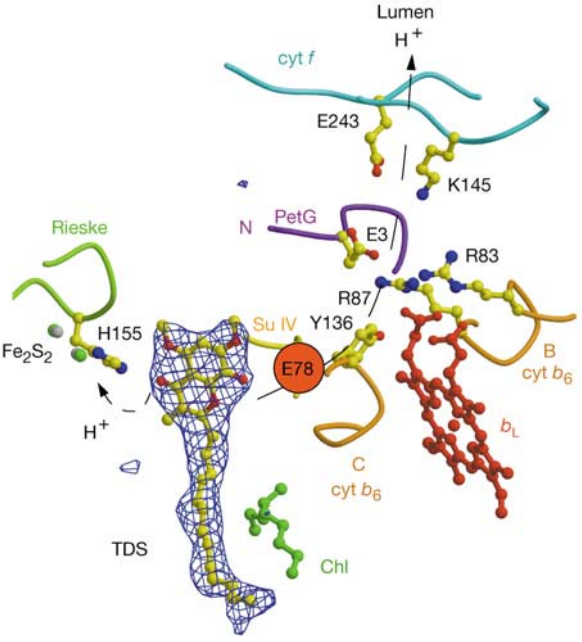

Figure 4 Q_o site with inhibitor. TDS is shown with a (F_o − F_c)-annealed omit map contoured at 5σ. Residue His 155 of the Rieske protein is within hydrogen-bonding distance of the carbonyl of TDS. To the right of TDS is the region around the lobe proximal to haem b_L, with the beginning of the low-potential chain and a possible channel for the second released proton. Charged residues are indicated (they are not hydrogen-bound; the distance between two neighbouring groups is about 5–6 Å, suggesting intervening water molecules). The conformation of cytochrome b_6 Tyr 136 differs from that in cytochrome bc_1. Su IV, subunit IV.

proximal lobe the main chain undergoes, between residues 58 and 63 of subunit IV, an 8 Å shift relative to the mitochondrial complex, making space for the amino terminus of PetG and modifying the distribution of charged residues, implying different paths for proton escape[30] (Fig. 4).

An additional haem on the stromal face at the Q_i site

The Q_i site is located on the stromal face, where proton uptake and reduction of plastoquinone (PQ) take place. It opens onto the hydrophobic groove at the dimer interface, as in cytochrome bc_1, but the active site is different. Indeed, a large, flat electron density, with two lateral extensions and an electron dense region at its centre (Fig. 1a), blocks access to haem b_H. This density can be attributed to a haem on the following grounds: (1) the strong density at its centre originates from an iron atom, as shown by anomalous Fourier maps calculated from data collected at several wavelengths (1.009, 1.215 and 1.738 Å), and by a difference Fourier map between two data sets taken at and near the absorption edge of the iron Kα transition (Fig. 5a). (2) The general shape of the electron density resembles that of the three known haems, with well-defined densities for the propionates (Fig. 1). (3) One vinyl group of the proposed haem is within bonding distance of the sulphur atom of Cys 35 from cytochrome b_6, consistent with the presence of a thioether bridge. The additional haem, therefore, must belong to the *c* group, and will henceforth be called haem c_i; however, the consensus sequence CXnCH or AXnCH is lacking. Although uncommon, haem attachment by a single thioether bridge has been reported previously[31]. (4) Pyridine haemochromogen spectra (data not shown) are consistent with the presence of an additional haem with one thioether bridge[31,32].

The discovery of an additional haem in an extensively studied complex was not anticipated. Nevertheless, there were clues to the presence of a covalently bound haem: (1) it explains the peroxidase activity of cytochrome b_6 in SDS–polyacrylamide gel electrophoresis gels[33], which is not observed with cytochrome bc_1; (2) it accounts for the excess mass of cytochrome b_6 in mass spectrometry experiments[34]; and (3) it is consistent with the involvement of four nuclear genes in haem binding to *C. reinhardtii*'s cytochrome b_6 (ref. 35).

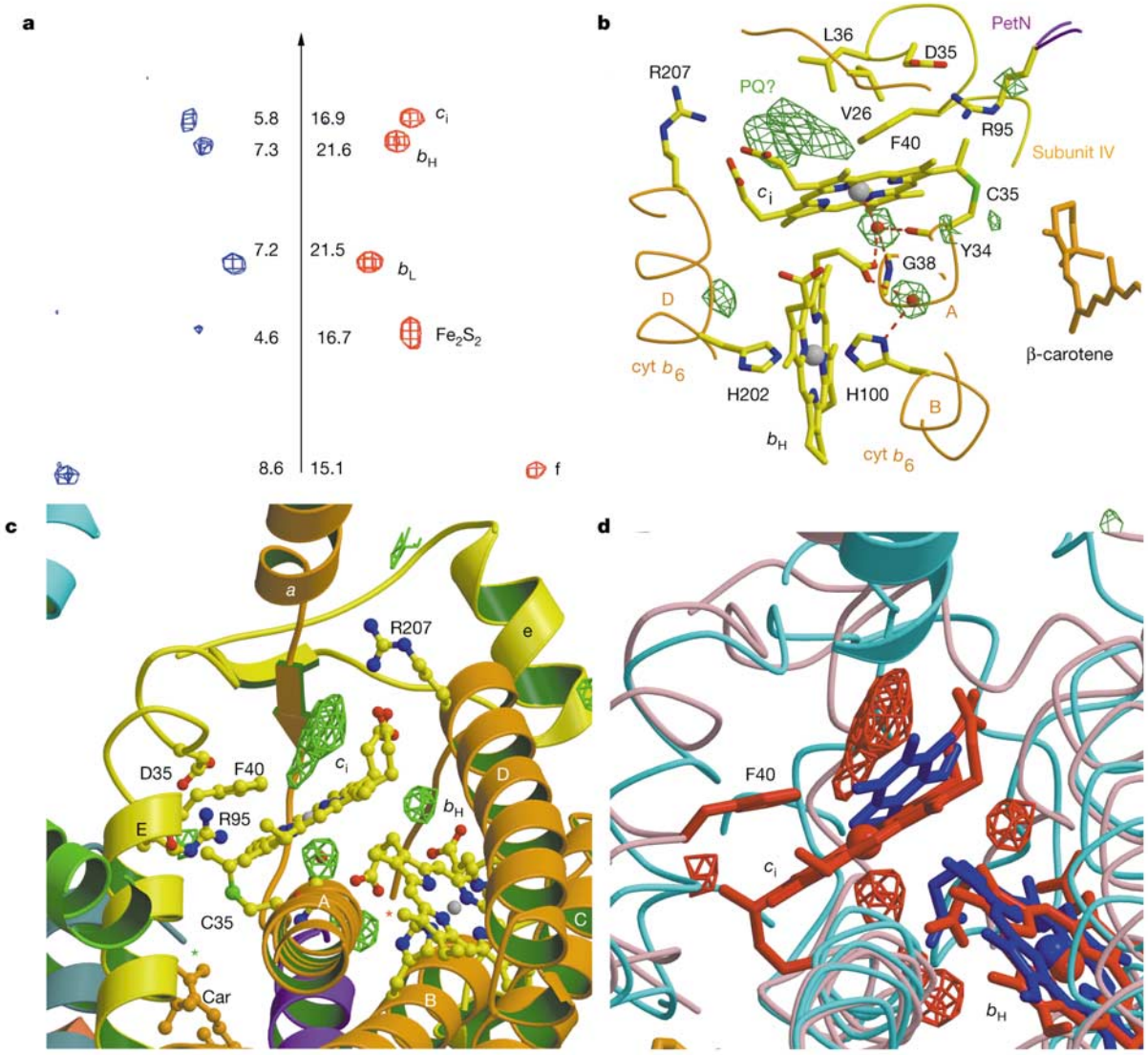

Figure 5 Q_i site. **a**, Irons in the dimer. Left, anomalous Fourier difference map ($\Delta f'$) at the iron edge (1.737–1.7408 Å) contoured at 4.0σ; right, anomalous map ($\Delta f''$) at 1.7389 Å contoured at 8.5σ. The arrow represents the two-fold axis. Peak height units are in σ. **b**, Haem c_i environment. The ($F_o - F_c$) map contoured at 5σ (in green) shows potential ligand and water molecules around haem c_i (also visible in **c** (green) and **d** (red)). **c**, Q_i site from the dimer interface. Red and green asterisks mark the C termini of cytochrome b_6 and PetN, respectively. *a*, N-terminal transverse helix of cytochrome b_6; Car, β-carotene. **d**, Superposition of cytochrome b_6f (red) and cytochrome bc_1 (PDB entry 1KB9; ref. 22) (blue) in the Q_i region. In cytochrome bc_1, haem b_H and an ubiquinone are depicted.

Axial ligands

The atypical character of haem c_i is accentuated by the unusual coordination of the iron atom, which does not directly interact with any amino acid. On its face close to b_H, Fourier differences maps ($F_o - F_c$) reveal the presence of an extra density, compatible with either a water molecule or an hydroxide ion (Fig. 5b), located within hydrogen-bonding distance of the carboxyl group of one propionate of haem b_H, the main-chain carbonyl of Tyr 34 and the amide of Gly 38 of cytochrome *b*. The same propionic carboxyl in turn is within hydrogen-bonding distance of another buried water molecule—also present in cytochrome bc_1 (ref. 22)—which itself can form a hydrogen bond with the Nδ atom of His 100, an axial ligand of haem b_H. The other face of haem c_i lines the active site pocket, where a weak electron density could be accounted for by either PQ or another ligand (Fig. 5b, c).

A haem with no axial amino acid ligand has never been observed in wild-type proteins, but it has been created by mutagenesis of myoglobin[36] or peroxidases[37]. Haem c_i should belong to the c' group (that is high-spin), whose broad spectral bands in the visible region of the spectrum ought to be dominated by those of the low-spin haems and other chromophores of the cytochrome b_6f. The agreement between linear dichroism spectra[38] and the orientation of haems *f*, b_L and b_H in the present structure bears witness to the proper assignment of their absorption bands. Electron paramagnetic resonance (EPR) spectra of purified b_6f samples do feature high-spin components[39], which would be consistent with the presence of a c'-type haem. However, as haems b_H and c_i are in van der Waals contact (Fig. 3), both haems could be EPR-silent.

Q_i site

The polypeptide chain around Q_i has the same topology as in cytochrome bc_1, but the active site has to accommodate a substrate and haem c_i, thus forming a different active site and explaining the lack of inhibitory effect of antimycin on cytochrome b_6f. Indeed, the amphipathic helix *a* of cytochrome b_6, which lies at the dimer interface parallel with the membrane plane (Fig. 2c), is shifted by about 6 Å towards the stroma relative to that in cytochrome bc_1 (Fig. 5c, d). This creates, adjacent to haem c_i, a pocket that is large enough for a substrate to interact with the haem plane, and, possibly, with the iron itself. This configuration differs from all known quinone-binding sites. Residue Phe 40 from subunit IV is in van der Waals' contact with the haem plane. Its role may be to control interaction of ligands with the haem iron. Near the entrance of the active site cavity one propionate of haem c_i is within hydrogen-bonding distance of Arg 207 at the carboxy-terminal end of helix D (His 202 in cytochrome bc_1). This residue is in a favourable position to interact with a quinone in the pocket.

Haem c_i and phylogenesis of cytochrome b_6-type complexes

The presence of an additional haem in the Q_i site ought to be a general feature of all cytochrome b_6f-like complexes. Indeed, Cys 35 of cytochrome b_6—to which haem c_i is covalently bound—as well as other amino acids of the Q_i pocket are well conserved in all chloroplast and cyanobacterial cytochrome b_6f complexes. No cysteine is present at that position in mitochondrial and most bacterial bc_1 cytochromes. It is, however, encountered in menaquinol:cytochrome *c* oxidoreductase from some members of the Firmicutes phylum (but not the Chlorobiaceae), such as *Bacillus subtilis*[40], *Heliobacillus mobilis* or *Heliobacterium gestii*; the latter two are photosynthetic and harbour a PSI-like reaction centre. The same pattern is found in this complex from these species: cytochrome *b* is split into cytochrome b_6 and subunit IV, subunit IV is predicted to feature three transmembrane helices, and the two haem-liganding histidines of helix D are separated by 14 amino acids[41]. It is not clear from the structure whether there is a necessity for having a split cytochrome *b*, but it could be a constraint from the haem c_i insertion machinery. Firmicutes and cyanobacteria are not that distant in evolutionary terms. Photosynthetic organisms that potentially harbour haem c_i all have a PSI-like reaction centre, and could function in a cyclic mode of electron transfer. Therefore, it is tempting to assign c_i to that role, even though direct evidence is lacking. In the non-photosynthetic Firmicutes there is a seven-residue insertion between residues 31 and 32 of cytochrome b_6, which might modify or obstruct a potential path for electron re-injection from the stroma site to Q_i (see below). There is, however, one noticeable outlier; the evolutionarily distant proteobacterium *Xylella fastidiosa* exhibits a cysteine equivalent to Cys 35 and an unsplit cytochrome *b*, but it is unclear whether a haem c_i is present, as the amino acids that would surround it have a mixed b_6/b pattern.

Functional implications

Haem c_i blocks quinone access to b_H. This intermediate position suggests its participation in electron flow from b_H to PQ, either as a 'wire' between b_H and PQ, or as a redox carrier. Indeed, in contrast with the bc_1 complex, light-induced electron injection in the low-potential chain of the b_6f complex under oxidizing conditions results in the reduction of only a fraction (up to 0.7) of b_H, without the corresponding formation of a detectable semiquinone species[42] (note however that the proximity of haem c_i would influence the EPR signal of a hypothetical semiquinone). Electron sharing between b_H and c_i might explain the fate of the missing electrons. In keeping with this hypothesis, ref. 5 established the existence of a carrier called G in *Chlorella sorokiniana* whose potential would be close to that of b_H and whose characteristics agree with the present structure. At present it needs to be demonstrated whether haem c_i is G. The accessibility of haem c_i from the stroma makes it a good candidate to participate in cyclic electron flow around PSI. Direct access to the Q_i site from the stroma is only prevented by the presence of Asp 35 (from subunit IV) and Arg 95 (from PetN) (Fig. 5b). Therefore, the existence of haem c_i brings further support to the idea that the re-injection of electrons occurs through cytochrome b_6f, even if details of the pathway from PSI remain unclear.

Untangling the interactions between the two Q_i haems will require close examination. Because a propionate of b_H interacts with the haem iron of haem c_i through an intervening water molecule or hydroxide ion, and because the p*K* of propionate is influenced by the redox state of b_H, the latter can modulate the redox state of haem c_i and, possibly, change the protonation state of the intervening molecule. This may be the heart of a proton pump.

The structure of a cyanobacterial cytochrome b_6f has been published during the revision of the present article[43]. Among others, differences exist concerning the mode of TDS binding, and hence the position of the Rieske protein, and the assignment of subunits PetG, PetL and PetN. □

Methods

Protein purification

Chlamydomonas reinhardtii was genetically modified in order to add a six-histidine tag at the C terminus of cytochrome *f* (ref. 27). Thylakoid membranes were solubilized with dodecyl-β-maltoside (DDM, Anatrace). After centrifugation, the supernatant was loaded onto an anion-exchange column (Source 30Q, Amersham), equilibrated with 20 mM Tris-HCl pH 8 and 1 mM DDM. Elution was carried out with 220 mM NaCl in the presence of 0.5 mM DDM. The eluate was loaded onto a 1-ml nickel column (HiTrap chelating, Amersham) equilibrated with 20 mM Tris-HCl pH 8, 250 mM NaCl, 0.3 mM DDM. The detergent concentration was reduced to 0.2 mM and the protein eluted with 300 mM imidazole. After desalting, the protein was concentrated to 10 $g\,l^{-1}$ by ultrafiltration (Microcon YM100, Millipore). Pyridine haemochromogen spectra were measured according to ref. 32. TDS was synthesized according to ref. 44.

Crystallization

Crystals were obtained by vapour diffusion (hanging drops) after addition of TDS (2:1 molar ratio of inhibitor to protein), the reservoir composition being 40 mM Tris-HCl pH 8, 40 mM NaCl, 0.2 mM DDM, 30% (w/v) glycerol and 25% (w/v) polyethylene glycol monomethylether (molecular mass 350 Da) (Fluka).

Crystallography

Data were collected at 70–100 K on the synchrotron beamline BM30A (CRG FIP) of the ESRF, and processed with the CCP4 package[45]. The space group of the crystal is *I*222. The solvent content is 82% of the crystal volume. Phases were obtained by multiple isomorphous replacement (see Supplementary Information) using crystals soaked in either 0.2 mM $HgCl_2$ or 2 mM $TbNO_3$. Heavy atoms were localized using SHELXD. Phases were refined with MLPHARE from the CCP4 package and improved by solvent modification using DM. The resulting electron density map allowed localizing the transmembrane helices and cytochrome *f*, whose extramembrane domain was replaced with the model of the soluble fragment from *C. reinhardtii* (Protein Data Bank (PDB) file 1E2W)[46]. Heavy-atom phases were combined with model phases of cytochrome *f* with SIGMAA and solvent flattened with DM. The model was built with the program O (ref. 47) (Hg binding to Cys 7 of PetG and Cys 81 of PetN confirmed the localization of these small subunits) and the structure was refined with CNS[48]. Figures were drawn with MOLSCRIPT[49] and RASTER3D[50].

Received 22 August; accepted 28 October 2003; doi:10.1038/nature02155.

1. Mitchell, P. Possible molecular mechanisms of the protomotive function of cytochrome systems. *J. Theor. Biol.* **62,** 327–367 (1976).
2. Crofts, A. & Wraight, C. A. The electrochemical domain of photosynthesis. *Biochim. Biophys. Acta* **726,** 149–185 (1983).
3. Sazanov, L. A., Burrows, P. A. & Nixon, P. J. The plastid *ndh* genes code for an NADH-specific dehydrogenase: isolation of a complex I analogue from pea thylakoid membranes. *Proc. Natl Acad. Sci. USA* **95,** 1319–1324 (1998).
4. Zhang, H., Whitelegge, J. P. & Cramer, W. A. Ferredoxin:$NADP^+$ oxidoreductase is a subunit of the chloroplast cytochrome b_6f complex. *J. Biol. Chem.* **276,** 38159–38165 (2001).
5. Lavergne, J. Membrane potential-dependant reduction of cytochrome b_6 in an algal mutant lacking photosystem I centers. *Biochim. Biophys. Acta* **725,** 25–33 (1983).
6. Joliot, P. & Joliot, A. The low potential electron transfer chain in cytochrome *b*/*f* complex. *Biochim. Biophys. Acta* **933,** 319–333 (1988).
7. Depege, N., Bellafiore, S. & Rochaix, J.-D. Role of chloroplast protein kinase Stt7 in LHCII phosphorylation and state transition in *Chlamydomonas*. *Science* **299,** 1572–1575 (2003).
8. Wollman, F.-A. State transitions reveal the dynamics and flexibility of the photosynthetic apparatus. *EMBO J.* **20,** 3623–3630 (2001).
9. Joliot, P. & Joliot, A. *In vivo* analysis of the effect of dicyclohexylcarbodiimide on electron and proton transfers in cytochrome *bf* complex of *Chlorella sorokiniana*. *Biochemistry* **37,** 10404–10410 (1998).
10. Pierre, Y. *et al.* On the presence and role of a molecule of chlorophyll *a* in the cytochrome b_6f complex. *J. Biol. Chem.* **272,** 21901–21908 (1997).
11. Xia, D. *et al.* Crystal structure of the cytochrome bc_1 complex from bovine heart mitochondria. *Science* **277,** 60–66 (1997).
12. Zhang, Z. *et al.* Electron transfer by domain movement in cytochrome bc_1. *Nature* **392,** 677–684 (1998).
13. Iwata, S. *et al.* Complete structure of the 11-subunit bovine mitochondrial cytochrome bc_1 complex. *Science* **281,** 64–71 (1998).
14. Hunte, C., Koepke, J., Lange, C., Rossmanith, T. & Michel, H. Structure at 2.3 Å resolution of the cytochrome bc_1 complex from the yeast *Saccharomyces cerevisiae* co-crystallized with an antibody Fv fragment. *Struct. Fold Des.* **8,** 669–684 (2000).
15. Breyton, C., Tribet, C., Olive, J., Dubacq, J.-P. & Popot, J.-L. Dimer to monomer conversion of the cytochrome b_6f complex. Causes and consequences. *J. Biol. Chem.* **272,** 21892–21900 (1997).
16. Pierre, Y., Breyton, C., Kramer, D. & Popot, J.-L. Purification and characterization of the cytochrome b_6f complex from *Chlamydomonas reinhardtii*. *J. Biol. Chem.* **270,** 29342–29349 (1995).
17. Zhang, H., Kurisu, G., Smith, J. L. & Cramer, W. A. A defined protein-detergent-lipid complex for crystallization of integral membrane proteins: The cytochrome b_6f complex of oxygenic photosynthesis. *Proc. Natl Acad. Sci. USA* **100,** 5160–5163 (2003).
18. Breyton, C. The cytochrome b_6f complex: structural studies and comparison with the bc_1 complex. *Biochim. Biophys. Acta* **1459,** 467–474 (2000).
19. Martinez, S. E., Huang, D., Szczepaniak, A., Cramer, W. A. & Smith, J. L. Crystal structure of chloroplast cytochrome *f* reveals a novel cytochrome fold and unexpected heme ligation. *Structure* **2,** 95–105 (1994).
20. Darrouzet, E., Moser, C. C., Dutton, P. L. & Daldal, F. Large scale domain movement in cytochrome bc_1: a new device for electron transfer in proteins. *Trends Biochem. Sci.* **26,** 445–451 (2001).
21. Carrell, C. J., Zhang, H., Cramer, W. A. & Smith, J. L. Biological identity and diversity in photosynthesis and respiration: structure of the lumen-side domain of the chloroplast Rieske protein. *Structure* **5,** 1613–1625 (1997).
22. Lange, C., Nett, J. H., Trumpower, B. L. & Hunte, C. Specific roles of protein-phospholipid interactions in the yeast cytochrome bc_1 complex structure. *EMBO J.* **20,** 6591–6600 (2001).
23. Zhang, H., Huang, D. & Cramer, W. A. Stoichiometrically bound β-carotene in the cytochrome b_6f complex of oxygenic photosynthesis protects against oxygen damage. *J. Biol. Chem.* **274,** 1581–1587 (1999).
24. Yan, J., Liu, Y., Mao, D., Li, L. & Kuang, T. The presence of 9-cis-β-carotene in cytochrome b_6f complex from spinach. *Biochim. Biophys. Acta* **1506,** 182–188 (2001).
25. Peterman, E. J. *et al.* Fluorescence and absorption spectroscopy of the weakly fluorescent chlorophyll *a* in cytochrome b_6f of Synechocystis PCC6803. *Biophys. J.* **75,** 389–398 (1998).
26. Hart, S. E., Schlarb-Ridley, B. G., Delon, C., Bendall, D. S. & Howe, C. J. Role of charges on cytochrome *f* from the cyanobacterium *Phormidium laminosum* in its interaction with plastocyanin. *Biochemistry* **42,** 4829–4836 (2003).
27. Choquet, Y., Zito, F., Wostrikoff, K. & Wollman, F.-A. Cytochrome *f* translation in *Chlamydomonas* chloroplast is autoregulated by its carboxyl-terminal domain. *Plant Cell* **15,** 1443–1454 (2003).
28. Crofts, A. R. *et al.* Pathways for proton release during ubihydroquinone oxidation by the bc_1 complex. *Proc. Natl Acad. Sci. USA* **96,** 10021–10026 (1999).
29. Zito, F., Finazzi, G., Joliot, P. & Wollman, F.-A. Glu78, from the conserved PEWY sequence of subunit IV, has a key function in cytochrome b_6f turnover. *Biochemistry* **37,** 10395–10403 (1998).
30. Finazzi, G. Redox-coupled proton pumping activity in cytochrome b_6f, as evidenced by the pH dependence of electron transfer in whole cells of *Chlamydomonas reinhardtii*. *Biochemistry* **41,** 7475–7482 (2002).
31. Mukai, K. *et al.* An atypical heme-binding structure of cytochrome c_1 of *Euglena gracilis* mitochondrial complex III. *Eur. J. Biochem.* **178,** 649–656 (1989).
32. Berry, E. A. & Trumpower, B. L. Simultaneous determination of hemes *a*, *b*, and *c* from pyridine hemochrome spectra. *Anal. Biochem.* **161,** 1–15 (1987).
33. Hurt, E. & Hauska, G. A cytochrome f/b_6 complex of five polypeptides with plastoquinol-plastocyanin-oxidoreductase activity from spinach chloroplasts. *Eur. J. Biochem.* **117,** 591–595 (1981).
34. Whitelegge, J. P., Zhang, H., Aguilera, R., Taylor, R. M. & Cramer, W. A. Full subunit coverage liquid chromatography electrospray ionization mass spectrometry ($LCMS^+$) of an oligomeric membrane protein: cytochrome b_6f complex from spinach and the cyanobacterium *Mastigocladus laminosus*. *Mol. Cell Proteom.* **1,** 816–827 (2002).
35. Kuras, R. *et al.* Molecular genetic identification of a pathway for heme binding to cytochrome b_6. *J. Biol. Chem.* **272,** 32427–32435 (1997).
36. Pond, A. E. *et al.* Assignment of the heme axial ligand(s) for the ferric myoglobin (H93G) and heme oxygenase (H25A) cavity mutants as oxygen donors using magnetic circular dichroism. *Biochemistry* **38,** 7601–7608 (1999).
37. Hirst, J. *et al.* Replacement of the axial histidine ligand with imidazole in cytochrome c peroxidase. 2. Effects on heme coordination and function. *Biochemistry* **40,** 1274–1283 (2001).
38. Schoepp, B., Chabaud, E., Breyton, C., Vermeglio, A. & Popot, J.-L. On the spatial organization of hemes and chlorophyll in cytochrome b_6f. A linear and circular dichroism study. *J. Biol. Chem.* **275,** 5275–5283 (2000).
39. Nitschke, W. & Hauska, G. On the nature of the g = 6 EPR signal in isolated cytochrome b_6f complex from spinach chloroplasts. *Biochim. Biophys. Acta* **892,** 314–319 (1987).
40. Yu, J. & Le Brun, N. E. Studies of the cytochrome subunits of menaquinone:cytochrome *c* reductase (*bc* complex) of *Bacillus subtilis*. Evidence for the covalent attachment of heme to the cytochrome *b* subunit. *J. Biol. Chem.* **273,** 8860–8866 (1998).
41. Schütz, M. *et al.* Early evolution of cytochrome *bc* complexes. *J. Mol. Biol.* **300,** 663–675 (2000).
42. Hope, A. B. The chloroplast cytochrome *bf* complex: a critical focus on function. *Biochim. Biophys. Acta* **1143,** 1–22 (1993).
43. Kurisu, G., Zhang, H., Smith, J. L. & Cramer, W. A. Structure of the cytochrome b_6f complex of oxygenic photosynthesis: Tuning the cavity. *Science*, 2 October 2003 (doi:10.1126/science.1090165).
44. Höffle, G., Kunze, B., Zorzin, C. & Reichenbach, H. Antibiotica aus gleitende Bakterien XIII:Stigmatellin A und B—zwei neue Antibiotika aus *Stigmatella aurantiaca* (Myxobacterales). *Liebigs Annal. Chem.* **12,** 1883–1904 (1984).
45. The CCP4 suite: Programs for protein crystallography. *Acta Crystallogr. D* **50,** 760–763 (1994).
46. Sainz, G. *et al.* Interruption of the internal water chain of cytochrome *f* impairs photosynthetic function. *Biochemistry* **39,** 9164–9173 (2000).
47. Jones, T. A., Zou, J. Y., Cowan, S. W. & Kjeldgaard, M. Improved methods for building protein models in electron density maps and the location of errors in these models. *Acta Crystallogr. A* **47,** 110–119 (1991).
48. Brünger, A. T. *et al.* Crystallography & NMR system: A new software suite for macromolecular structure determination. *Acta Crystallogr. D* **54,** 905–921 (1998).
49. Kraulis, P. J. A program to produce both detailed and schematic plots of protein structures. *J. Appl. Crystallogr.* **24,** 946–950 (1991).
50. Merritt, E. & Bacon, D. Raster3D photorealistic molecular graphics. *Methods Enzymol.* **277,** 505–524 (1997).
51. Murakami, S. & Packer, L. Protonation and chloroplast membrane structure. *J. Cell Biol.* **47,** 332–351 (1970).

Supplementary Information accompanies the paper on **www.nature.com/nature**.

Acknowledgements We thank the local contacts of beamline BM30 (ESRF, CRG FIP) J.-L. Ferrer, R. Kahn and P. Carpentier for assistance in data collection; C. Lebreton for membrane preparations; P. Hervé and P. Fellmann for the synthesis of TDS; Y. Pierre, F. Zito and C. Breyton for biochemical expertise; P. Joliot, J. Lavergne, F. Daldal, F. Baymann, W. Nitschke and G. Ajlani for discussions; and C. Breyton, G. Finazzi and A. A. Pascal for discussions and critical reading of the manuscript. This work was supported by the CNRS and Paris-7 University.

Competing interests statement The authors declare that they have no competing financial interests.

Correspondence and requests for materials should be addressed to D.P. (Daniel.Picot@ibpc.fr) or J.-L.P. (Jean-Luc.Popot@ibpc.fr). Coordinates and structure factors have been deposited with the PDB under accession code 1Q90.

